Molecular Scale Dynamics of Large Ring Polymers

S. Gooßen,[1,*] A. R. Brás,[1] M. Krutyeva,[1] M. Sharp,[2] P. Falus,[2] A. Feoktystov,[3] U. Gasser,[4]
W. Pyckhout-Hintzen,[1] A. Wischnewski,[1] and D. Richter[1]
[1]*Jülich Centre for Neutron Science (JCNS-1) and Institute for Complex Systems (ICS-1),*
Forschungszentrum Jülich GmbH, 52425 Jülich, Germany
[2]*Institute Laue-Langevin (ILL), 38042 Grenoble Cedex 9, France*
[3]*Jülich Centre for Neutron Science (JCNS), Forschungszentrum Jülich GmbH,*
Outstation at MLZ, Lichtenbergstraße 1, 85747 Garching, Germany
[4]*Laboratory for Neutron Scattering and Imaging, Paul Scherrer Institut, 5232 Villigen, Switzerland*

(Received 9 May 2014; revised manuscript received 11 July 2014; published 14 October 2014)

We present neutron scattering data on the structure and dynamics of melts from polyethylene oxide rings with molecular weights up to ten times the entanglement mass of the linear counterpart. The data reveal a very compact conformation displaying a structure approaching a mass fractal, as hypothesized by recent simulation work. The dynamics is characterized by a fast Rouse relaxation of subunits (loops) and a slower dynamics displaying a lattice animal-like loop displacement. The loop size is an intrinsic property of the ring architecture and is independent of molecular weight. This is the first experimental observation of the space-time evolution of segmental motion in ring polymers illustrating the dynamic consequences of their topology that is unique among all polymeric systems of any other known architecture.

DOI: 10.1103/PhysRevLett.113.168302 PACS numbers: 82.35.Lr, 29.30.Hs, 61.05.fg, 83.80.Sg

From a topological point of view among all polymer architectures, polymer rings are unique since rings are closed structures without ends. In dense melts, this feature significantly influences both ring conformations and dynamics [1–12]. Interpenetration of ring polymers is entropically hindered and therefore rings are predicted to prefer the conformations of a crumpled globule [13] or that of a lattice animal [14]. For the dynamics this has severe consequences: Within the tube confinement by surrounding chains, linear chains relax by leaving their initial tube [15]. Branched polymers relax by back folding the branches against entropic barriers [16]. In all of these processes the chain ends play the essential role. Due to their particular topology, for rings such processes are impossible and a full understanding of the dynamics remains a challenge to polymer physics motivating the great current interest in such polymers.

In equilibrium crumpled globules have been proposed where subchains form loops, leading to a fractal dimension $d_f = 3$ with close similarity to the folding of chromatin fibers in the cell nucleus [17–19]. Synthetic ring polymers may be considered as models for the chromatin behavior and their understanding will also promote a deeper insight into the chromatin problem. Since the synthesis of well-defined and pure large ring polymers is highly demanding, there has been a focus recently on simulations of their structure and dynamics [20–23].

Neglecting topological confinement and assuming pure entropy driven Rouse dynamics, a theoretical approach to ring dynamics was presented in terms of a modified Rouse model [24]. While adjusting the Rouse model to the ring architecture is straightforward, it does not account for any topological confinement effects. Recent MD studies on bead and spring rings by Halverson *et al.* [20] concluded a rather compact structure and an asymptotic conformation of a crumpled globule for large rings. The same authors unraveled a subdiffusive center of mass (c.m.) behavior $\langle r^2_{\mathrm{cm}}(t)\rangle \propto t^{3/4}$ at early times, before the transition to normal translational diffusion (D) takes place at about $\langle r^2_{\mathrm{cm}}\rangle = 2.5R^2_g$ [21]. At higher molecular weights, $D \propto N^{-2}$ (N: chain length) was found. A similar value was also obtained by Hur *et al.* [23] and agrees with a scaling approach by Rubinstein *et al.* [25]. Of note, focusing on the relaxation across a centrality bond deep inside the trunk of the ring lattice animal, a time dependence $t^{3/4}$ was again derived [22]. Regarding the segmental relaxation, simulations [21,23] observed a significant slowing down towards $\langle r^2_{\mathrm{seg}}(t)\rangle \propto t^{\nu}$, with $\nu = 0.25$ to 0.35. Such a power law is also characteristic for the local reptation regime, where the Rouse modes relax within the stiff confining tube yielding $\langle r^2_{\mathrm{seg}}(t)\rangle \propto t^{1/4}$. The reason for the occurrence of such a time regime for rings is unclear.

Employing small angle neutron scattering (SANS) and neutron spin echo (NSE) spectroscopy, in this Letter we present an analysis of the molecular structure and dynamics of large ring polymers in melts. We find (i) a tendency towards mass fractal behavior evolving systematically with increasing molecular weight, (ii) a subdiffusive c.m. motion at submolecular distances with mean squared displacement (m.s.d.) $\propto t^{3/4}$, (iii) at short times, ring sections or loops that relax like short unentangled chains, and (iv) at later times slow loop motion following a t^{ν} law with $\nu = 0.32$.

The experiments provide a first direct observation of the space-time evolution of segmental and c.m. motion in ring polymers at and below the scale of the ring and create a benchmark for simulations and theory.

Highly pure hydrogenous (h) and deuterated (d) polyethylene oxide (PEO) rings of two molecular weights were synthesized as described previously for a 5 K ring [10]. For the first pair of rings, $M_n = 10\,100$ g/mol (h) and $M_n = 11\,100$ g/mol (d) within an error of 3% was obtained by nuclear magnetic resonance. For simplification this ring is called the 10 K ring in the following. For the second pair, the 20 K ring, $M_n = 20\,100$ g/mol (h) and $M_n = 23\,200$ g/mol (d) was determined. Size exclusion chromatography revealed polydispersity indices $M_w/M_n \leq 1.03$ for all samples. Blends of h and d were prepared in solution and freeze dried from benzene. The volume fraction of the h polymers in h-d blends was 20% for the 10 K ring and 10% for the 20 K ring, respectively.

SANS experiments were performed at KWS-1 at MLZ (Munich, Germany) and SANS-II at SINQ (PSI Villigen, Switzerland). NSE studies were carried out at the spectrometer IN15 at the ILL (Grenoble, France). The measurements were performed at $T = 413$ K, well above the crystallization temperature that was found to be slightly lower than for the linear counterparts by differential scanning calorimetry (always below 340 K).

Figure 1 shows SANS data for the 5 K, 10 K, and 20 K rings in the representation $S(Q)Q^3$ versus QR_g. In the low QR_g regime, all data fall perfectly on one master curve if properly normalized for volume fraction and number of monomers N. As predicted by the crumpled globule picture and simulation [20], in the intermediate Q range a shoulder develops indicating an approach towards an asymptotic mass fractal behavior. With increasing N it becomes more pronounced and extended, indicating the increasing local compactness. This result is substantiated by the N dependence of R_g^2 that is plotted in the lower inset of Fig. 1. As found earlier [5–10], for all N the conformation is significantly more compact than the Gaussian prediction. For intermediate Q a power law behavior in the form factor following $Q^{-1/\nu}$, with $\nu = 0.43 \pm 0.015$, was obtained by fitting a modified Debye function [10]. From ν the N dependence of $R_g^2 \propto N^{2\nu}$ is derived and in the inset of Fig. 1 compared with R_g^2 from Guinier fits.

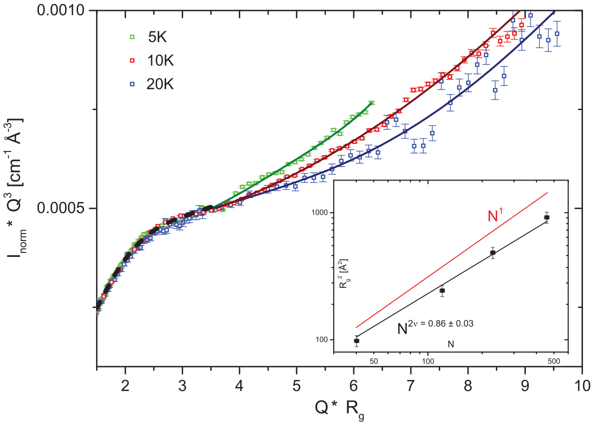

FIG. 1 (color). SANS data for the 5 K (green symbols), 10 K (red symbols), and 20 K (blue symbols) rings plotted versus QR_g. The data yield a perfect master curve in the low QR_g regime. The dashed black line up to $QR_g = 3.5$ represents a fit to the data, the colored lines in the high QR_g regime are guides for the eyes. The inset shows the N dependence of R_g^2 (red line: Gaussian expectation [26], black line: experimental data including one additional small 2 K PEO ring [9]).

Figure 2 presents the dynamic structure factors $S(Q,t)/S(Q)$ obtained by NSE over an exceptionally large time regime. These data reveal both the internal dynamics and the c.m. motion up to time scales where $\langle r_{\mathrm{cm}}^2 \rangle$ well exceeds R_g^2. The selection rules for internal modes of ring polymers (only even modes) [24] allow a direct observation of the c.m. m.s.d. at low Q. There, even for the largest ring internal modes do not contribute to $S(Q,t)$. Thus, a direct measurement of $\langle r_{\mathrm{cm}}^2(t) \rangle$ becomes possible via $S(Q,t)/S(Q) = \exp(-Q^2 \langle r_{\mathrm{cm}}^2(t) \rangle / 6)$. This is the Gaussian assumption, proven correct for the 10 K and 20 K rings by the Q dependence of the low Q spectra. Note that a pronounced non-Gaussian behavior was found for the c.m. motion of the 5 K ring [10].

Complementary pulsed field gradient (PFG) NMR data reveal the translational diffusion D in the milliseconds regime. They agree well with the NSE data and allow a good extrapolation of the crossover behavior for the highest N (solid colored lines in Fig. 3 in the t^1 regime). In Fig. 3 we present all c.m. m.s.d. for the different rings scaled with N versus time. At times just below those associated with the normal diffusion regime, all scaled data collapse to a single master curve displaying a subdiffusive c.m. motion with scaled m.s.d. proportional to $t^{3/4}$. The mass scaling seems to indicate purely friction controlled subdiffusive motion. However, for the two larger N, at still smaller times the time dependences are even weaker than $t^{3/4}$. A similar behavior was found by Milner *et al.* for the relaxation across the centrality bond at early times [22]. For the two higher molecular weights, D is compatible with $D \propto N^{-2}$ in agreement with simulation results as well as the scaling prediction of Rubinstein [25]. The crossover from subdiffusive to normal diffusion occurs at about $\tau_{\mathrm{cross}} \approx 2.5 R_g^2/D$ (10 K, 20 K rings, again in agreement with simulation [21]), while for the small 5 K ring this crossover is shifted towards 6 R_g^2. We note that this ring is also characterized by significant non-Gaussianity in the translational diffusion behavior, which has a maximum around $\tau_{\mathrm{cross}} = 2.5 R_g^2/D$ [10].

While the evaluation of the c.m. m.s.d. is straightforward, the access to the segmental motions (the internal dynamics) is much more involved and challenging. In the following we display the different steps needed in order to arrive at a consistent picture of the observations:

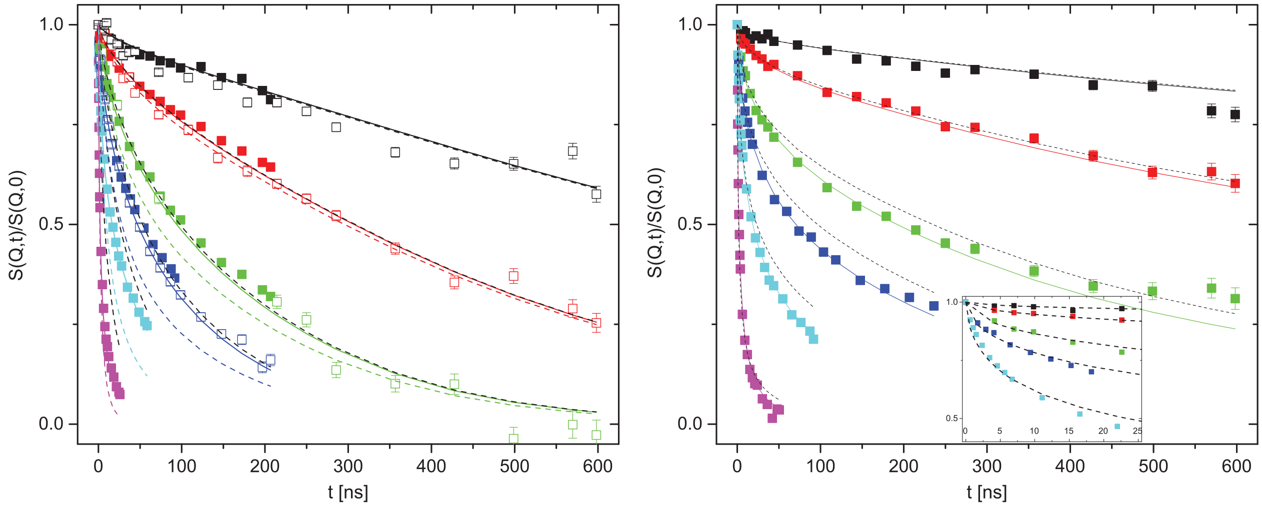

FIG. 2 (color). NSE spectra for the 10 K (left panel) and 20 K (right panel) ring for Q values (from top to down) 0.03, 0.05, 0.08, 0.1, 0.13, and 0.2 Å^{-1} at $T = 413$ K. Full and empty symbols (left panel) refer to two different wavelength setups. Lines and inset, see text.

Step 1: In the first step we parametrized the c.m. displacement illustrated in Fig. 3 to obtain an analytic form for $\langle r_{\mathrm{cm}}^2(t)\rangle$. With this, for all Q the contribution of the c.m. diffusion to $S(Q,t)$ can be calculated via $S(Q,t)/S(Q) = \exp(-Q^2\langle r_{\mathrm{cm}}^2(t)\rangle/6)$. The result is shown for the 10 K rings by the dashed black lines in Fig. 2 (left panel). For the four smallest Q values the c.m. m.s.d. perfectly describes $S(Q,t)$, thereby demonstrating the Gaussian character of the c.m. diffusion. At higher Q beyond the c.m. diffusion, an additional contribution of internal relaxation is observed.

Step 2: We evaluated the observed internal dynamics in terms of the Rouse structure factor for ring relaxation [Eq. (1), $p_{\min} = 2$]:

$$S(Q,t) = \frac{1}{N}\sum_{i,j}\exp\Bigg[-\frac{\langle r_{\mathrm{cm}}^2\rangle Q^2}{6} - \frac{1}{6}Q^2 l^2|i-j|^{2\nu} \times\left(1-\frac{|i-j|}{N}\right)^{2\nu} - \frac{4Q^2N^{2\nu}l^2}{6\pi^2}\sum_{p_{\min,\mathrm{even}}}^{N}\frac{1}{p^2}\cos\left(p\pi\frac{(i-j)}{N}\right)\left(1-\exp\frac{-tp^2}{\tau_R}\right) - F\frac{4Q^2N^{2\nu}l^2}{6\pi^2} \times\sum_{p,\mathrm{even}}^{p_{\min}-2}\frac{1}{p^2}\cos\left(p\pi\frac{(i-j)}{N}\right)\left(1-\exp\frac{-tp^4}{\tau_{\mathrm{cross}}}\right)\Bigg]. \quad (1)$$

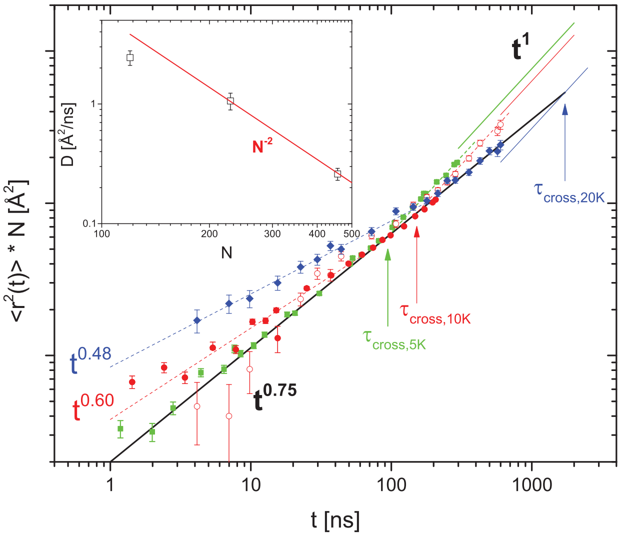

FIG. 3 (color). Center of mass mean squared displacement. N versus time for low $Q = 0.05$ Å^{-1} for the 5 K (green), 10 K (red) and 20 K (blue) rings. The inset shows the molecular weight dependence of the diffusion coefficient approaching $D \propto N^{-2}$ for high N.

With $p_{\min} = 2$ the last term vanishes and Eq. (1) yields the expression derived in [24]. Thereby, the well-known monomeric friction coefficient for PEO [27] was inserted that for rings should not depend on the molecular weight (no ends). The predicted relaxation is far too strong (see Fig. 2: left panel, dashed colored lines)—seemingly, not all of the Rouse modes are involved in the relaxation of the ring.

Step 3: In order to assess to what extent Rouse relaxation takes place we analyzed the data in terms of a reduced number of Rouse modes. Suppressing the first ring mode ($p = 2$) and activating all modes with $p \geq 4$—i.e., $p_{\min} = 4$—yields an excellent description of the data (the solid lines in Fig. 2, left panel). Note that $p_{\min}$ is the only free parameter. From the first active mode we may conclude that ring sections of about 60 monomers (i.e., $N/p_{\min}$) relax undisturbed by topological effects.

For the 20 K ring data we followed the same procedure. Again the spectra contain a substantial amount of segmental relaxation (step 1). Moreover, fitting the spectra at short times ($t < 20$ ns), a reduced number of active modes was again found, with $p_{\min} = 8$ [see Fig. 2 (right panel, dashed

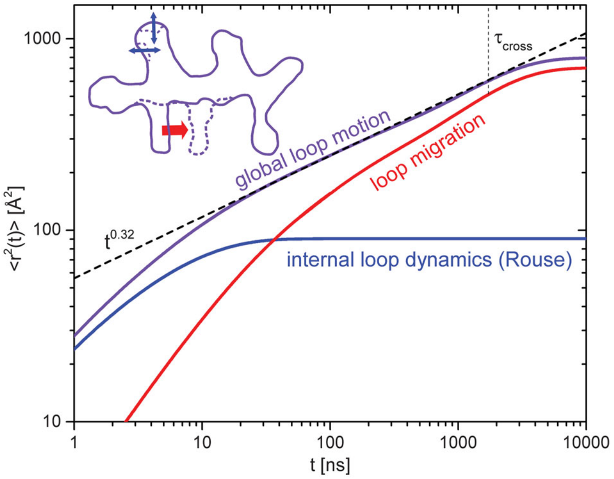

FIG. 4 (color). Time dependent m.s.d. of the 20 K ring. Blue line: loop relaxation at short times. Red line: dynamics of the loops derived from the motions of the slowly decaying low p modes. Purple line: sum of both with a slope of $t^{0.32}$ at intermediate times. This slope is indicated by the dashed black line.

lines)]. It is remarkable that this p_{min} again refers to a ring section of about 60 monomers that can relax without topological hindrance. The inset in Fig. 2 (right panel) shows that for short times the fit is excellent. However, this picture underestimates significantly the relaxation at longer times. In Fig. 2 (right panel) this is illustrated by the deviations from the model at times beyond 20 ns. A way out would be to allow longer wavelength modes, but this would significantly overpredict the decay at short times. Thus we conclude that further relaxation takes place; however, under significant constraints. We may interpret the result for the early time motion as a free Rouse relaxation of loops formed, e.g., in a lattice animal structure. These loops would have a molecular weight of about 2500 g/mol and are able to relax freely. Incidentally this loop size is comparable with the entanglement length for PEO of $M_e = 2000$ g/mol. While for the 10 K ring the picture of loop relaxation seems to be sufficient to describe the observed spectra, this is not the case for the 20 K ring. Here the loop relaxation alone underestimates the internal relaxation of the ring. In order to go further, we use the result of a recent simulation revealing a $t^{1/4}$ evolution of the ring segmental dynamics until the crossover to normal translational diffusion is reached [21]. Using the mode picture, in a phenomenological way such a $t^{1/4}$ behavior of the mean square displacement may be achieved in adapting the power law for the characteristic times τ_p from p^{-2} to p^{-4}. Generally and asymptotically, a p^{-n} power law for the mode relaxation leads to a m.s.d. proportional $t^{1/n}$.

This consideration suggests that, if we stay within a Rouse-type mode picture, for the lower mode numbers the dispersion for the characteristic times τ_p should change to p^{-4}. While for the fast Rouse like relaxation the basis time is given by the Rouse time τ_R, at this point a new basis time $\tau_{\mathrm{ring}} \approx \tau_{\mathrm{cross}}$ would come into play as a reference for the slower process. This time is known from the transition of the c.m. displacements to normal diffusion, as shown in Fig. 3. Fixing $\tau_{\mathrm{cross}} = 1725$ ns and fitting the range of spatial relaxation that is achievable for the internal motions of the ring, we obtain an extremely good fit of the 20 K ring data (see Fig. 2, right panel) predicting a maximum extent of the internal relaxation [F in Eq. (1)] of about 90% of R_g.

Finally, Fig. 4 displays the time dependent m.s.d. of the 20 K ring as it follows from the description of the dynamic structure factor. The blue line displays the time dependent loop relaxation at short times—it provides a steep increase related to the steep initial decay of the dynamic structure factor at high Q and then assumes a plateau displaying the spatial limit of the internal motions within the loop. The red line displays the dynamics of the loops derived from the motions of the slowly decaying low p modes. At short times this process is marginal, but at intermediate times it takes over and dominates the weaker power law for motion of the loops along the lattice animal. Finally, around τ_{cross} it saturates—from here on, translational diffusion of the whole ring takes over. The sum of the two processes in Fig. 4 yields a slope of 0.32 at intermediate times (dashed line) in almost perfect agreement with simulation [23] (slope 0.35).

Our experiments present unique insights into the structure and related dynamics of very well-defined ring polymers. With increasing molecular weight the structure systematically evolves towards a compact mass fractal structure. The combined approach employing space-time resolving NSE and diffusion sensitive PFG NMR provided three significant experimental insights: (i) NSE unraveled anomalous c.m. diffusion at the scale of the molecule. This motion, $\langle r_{\mathrm{cm}}^2(t) \rangle \propto t^{3/4}$, extends in space up to several times the ring radius of gyration and verifies recent simulation results. It is striking that the approach on the motion across the centrality bond even predicts the observed deviations from the $t^{3/4}$ law towards lower exponents at early times. (ii) The observed M_w dependence of D agrees well with both simulation and scaling theory. (iii) The most prominent result is the observation of topologically unconstrained loop motion with loop sizes independent of M_w. This provides a first experimental verification of theoretical models that invoke lattice animals or crumpled globules, where the loop size would be an intrinsic ring property. Beyond that, the 20 K data show that the loops are able to slowly migrate.

Our data verify a number of new extensive computer simulations and present a novel, conclusive interpretation of the microscopic dynamics measured by NSE.

This research project has been supported by the European Commission under the Seventh Framework Programme through the Research Infrastructures action of the Capacities Specific Programme, NMI3-II Grant No. 283883. The authors acknowledge financial support from the European Commission under the Seventh Framework Programme by means of the grant agreement for the Integrated Infrastructure Initiative No. 262348 European Soft Matter Infrastructure (ESMI).

---

[*] s.goossen@fz-juelich.de

[1] M. Kapnistos, M. Lang, D. Vlassopoulos, W. Pyckhout-Hintzen, D. Richter, D. Cho, T. Chang, and M. Rubinstein, Nat. Mater. **7**, 997 (2008).

[2] G. B. McKenna and D. J. Plazek, Polym. Commun. **27**, 304 (1986).

[3] J. Roovers, Macromolecules **21**, 1517 (1988).

[4] R. Pasquino, T. C. Vasilakopoulos, Y. C. Jeong, H. Lee, S. Rogers, G. Sakellariou, J. Allgaier, A. Takano, A. R. Brás, T. Chang, S. Gooßen, W. Pyckhout-Hintzen, A. Wischnewski, N. Hadjichristidis, D. Richter, M. Rubinstein, and D. Vlassopoulos, ACS Macro Lett. **2**, 874 (2013).

[5] S. Gagliardi, V. Arrighi, A. Dagger, and A. J. Semlyen, Appl. Phys. A **74**, s469 (2002).

[6] V. Arrighi, S. Gagliardi, A. C. Dagger, J. A. Semlyen, J. S. Higgins, and M. J. Shenton, Macromolecules **37**, 8057 (2004).

[7] S. Gagliardi, V. Arrighi, R. Ferguson, A. C. Dagger, J. A. Semlyen, and J. S. Higgins, J. Chem. Phys. **122**, 064904 (2005).

[8] G. Beaucage and A. S. Kulkarni, Macromolecules **43**, 532 (2010).

[9] A. R. Brás, R. Pasquino, T. Koukoulas, G. Tsolou, O. Holderer, A. Radulescu, J. Allgaier, V. G. Mavrantzas, W. Pyckhout-Hintzen, A. Wischnewski, D. Vlassopoulos, and D. Richter, Soft Matter **7**, 11169 (2011).

[10] R. Brás, S. Gooßen, M. Krutyeva, A. Radulescu, B. Farago, J. Allgaier, W. Pyckhout-Hintzen, A. Wischnewski, and D. Richter, Soft Matter **10**, 3649 (2014).

[11] P. C. Griffiths, P. Stilbs, G. E. Yu, and C. Booth, J. Chem. Phys. **99**, 16752 (1995).

[12] D. Kawaguchi, K. Masuoka, A. Takano, K. Tanaka, T. Nagamura, N. Torikai, R. M. Dalgliesh, S. Langridge, and Y. Matsushita, Macromolecules **39**, 5180 (2006).

[13] A. Y. Grosberg, S. K. Nechaev, and E. I. Shakhnovich, J. Phys. (Paris) **49**, 2095 (1988).

[14] M. Rubinstein, Phys. Rev. Lett. **57**, 3023 (1986).

[15] P. G. de Gennes, J. Chem. Phys. **55**, 572 (1971).

[16] T. C. B. McLeish, Adv. Phys. **51**, 1379 (2002).

[17] T. Cremer and C. Cremer, Nat. Rev. Genet. **2**, 292 (2001).

[18] A. Rosa and R. Everaers, PLoS Comput. Biol. **4**, e1000153 (2008).

[19] B. V. S. Iyer and G. Arya, Phys. Rev. E **86**, 011911 (2012).

[20] J. D. Halverson, W. B. Lee, G. S. Grest, A. Y. Grosberg, and K. Kremer, J. Chem. Phys. **134**, 204904 (2011).

[21] J. D. Halverson, W. B. Lee, G. S. Grest, A. Y. Grosberg, and K. Kremer, J. Chem. Phys. **134**, 204905 (2011).

[22] S. T. Milner and J. D. Newhall, Phys. Rev. Lett. **105**, 208302 (2010).

[23] K. Hur, R. G. Winkler, and D. Y. Yoon, Macromolecules **39**, 3975 (2006).

[24] G. Tsolou, N. Stratikis, C. Baig, P. S. Stephanou, and V. G. Mavrantzas, Macromolecules **43**, 10692 (2010).

[25] S. P. Obukhov, M. Rubinstein, and T. Duke, Phys. Rev. Lett. **73**, 1263 (1994).

[26] B. H. Zimm and W. H. Stockmayer, J. Chem. Phys. **17**, 1301 (1949).

[27] K. Niedzwiedz, A. Wischnewski, W. Pyckhout-Hintzen, J. Allgaier, D. Richter, and A. Faraone, Macromolecules **41**, 4866 (2008).